Macromolecules

ARTICLE

pubs.acs.org/Macromolecules

Phase Behavior and Color Tuning of Poly(4-vinylpyridine)-*b*-poly(ε-caprolactone) Complexed with Chromophores

Chien-Lin Li,[†] Ming-Chia Li,[†] and Rong-Ming Ho*[,†,‡]

[†]Department of Chemical Engineering, National Tsing Hua University, Hsinchu 30013, Taiwan

[‡]Frontier Reasearch Center on Fundamental and Applied Sciences of Matters

Supporting Information

ABSTRACT: A series of poly(4-vinylpyridine)-*b*-poly(ε-caprolactone) (P4VP-PCL) diblock copolymers have been synthesized and used for the formation of nanostructures with tunable colors arising from the association of chromophores with P4VP block in P4VP-PCL. The association of chromophores leads to the bathochromical shifts of charge transfer absorption peaks, resulting in the color appearance into the visible region. To achieve the formation of well-defined nanostructured materials, the phase behavior of the mixtures of chromophore/P4VP-PCL was systematically examined. As evidenced by transmission electron microscopy and small-angle X-ray scattering (SAXS), the phase transformation of self-assembled nanostructures can be easily induced by introducing chromophores due to the association of 2-methylidenepropanedinitrile in the chromophores with the lone-pair electron of nitrogen in P4VP block (that is the increase on the effective volume fraction of P4VP, as identified by SAXS experiments through the analysis of one-dimensional correlation function). As a result, by taking advantage of charge transfer and corresponding morphologies from transformation, well-defined nanostructured films resulting from mixing of chromophore and P4VP-PCL offer the possibility to create stimuli-responsive nanomaterials with tunable color.

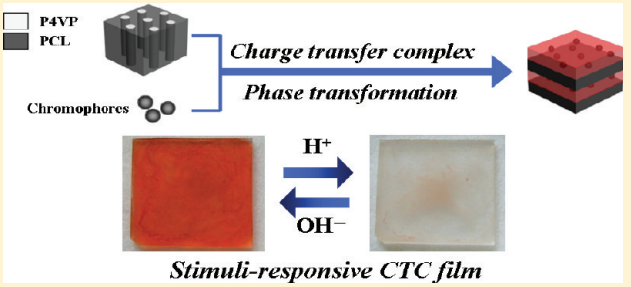

INTRODUCTION

In soft matter, block copolymers (BCPs) are a natural choice when aiming for nanostructures formed by a simple self-assembly process.[1−10] The covalent links between chemically different blocks prevent macrophase separation which otherwise would result from unfavorable interactions. Microphase separation is thus driven by the balance of the enthalpy of demixing of the constituted components of BCPs. For a diblock copolymer, the volume fraction of one component controls which ordered nanostructures are accessed beneath the order−disorder transition.[1] Many applications of BCPs could emerge due to differences in the chemical or physical properties of constituted blocks. Association with species, such as homopolymers, nanoparticles, and small molecules, selectively into BCP domains is advantageous as it not only imparts a desired functionality but can also be used to alter morphology and domain spacing without a need for synthesis of new BCPs. Consequently, extensive studies have focused on the incorporation of homopolymers with BCPs in which the observed phase behavior of the blends was found to be dependent upon the composition and chain length of homopolymer. The phase behavior of homopolymer/BCP blends has been thoroughly examined and suggested that low-molecular-weight PS homopolymers can be uniformly solubilized into the corresponding microdomain because of favorable entropy of mixing.[11] By contrast, larger homopolymers would be localized at the center of the incorporating block to minimize the loss in entropy caused by stretching of the BCP and homopolymer chains.

The phase behavior of inorganic materials within BCPs is usually achieved by introducing specific interactions between inorganic and organic constituents. For instance, through hybridization, mercaptoacetic acid-modified CdS nanoparticles can be selectively dispersed in P4VP microdomains of polystyrene-*b*-poly(4-vinylpyridine) (PS-P4VP) as a result of the formation of hydrogen bonding between the P4VP block and modified CdS nanoparticles. This process in turn induces a morphological transformation from a hexagonally packed cylinder phase into a lamellar phase.[12] Moreover, the phase transformation of polystyrene-*b*-poly(2-vinylpyridine) (PS-P2VP) from original lamellae to sphere and disorder can be found by introducing modified gold nanoparticles.[13] By contrast, disorder to order transition in lithium salts/polystyrene-*b*-poly(methyl methacrylate) (PS-PMMA) hybrids can be achieved by directly blending inorganic precursors and BCPs, suggesting that the overall segmental interaction, especially for entropic part, would significantly increase as a result of ionic complex formation.[14,15] Our previous studies in the Au^{3+}/poly(4-vinylpyridine)-*b*-poly(ε-caprolactone) (P4VP-PCL) hybrids indicated that morphological evolution can be observed by introducing a small amount of gold precursors preferentially associated with the P4VP due to significant increase in effective

Received: July 27, 2011
Revised: September 28, 2011
Published: October 20, 2011

Table 1. Characterization of P4VP-PCL BCPs

sample	M_n^{P4VP} (g/mol)[a]	M_n^{PCL} (g/mol)[a]	M_n^{total} (g/mol)	$f_{P4VP}{}^{v}$	PDI[b]	morphology
V2C7	2000	7000	9000	0.24	1.25	cylinder
V4C7	4000	7000	11000	0.37	1.24	cylinder
V5C10	5700	10900	16600	0.40	1.25	lamellar

[a] M_n^{P4VP} and M_n^{PCL} were characterized by proton nuclear magnetic resonance (^{1}H NMR). [b] The polydispersity index (PDI) in the diblock copolymers was determined by GPC using PS as a standard calibration.[17,49]

excluded volume of P4VP block.[16,17] Also, the PCL block of the P4VP-PCL plays an important role to stabilize the phase behavior of hybrids so as to prevent the occurrence of disorder nanostructures during hybridization.[17]

Similarly, a rich phase behavior can be acquired by selectively associating organic molecules with phase-separated microdomain of BCPs. It offers appealing applications in nanotechnologies to acquire nanostructured materials with responsive properties by taking advantage of association/dissociation processes. Association of different species to polymers can be achieved by using ionic interaction,[18−27] coordination,[28−36] hydrogen bonding,[37−44] and charge transfer.[45−48] Chromophore is the part of a molecule responsible for its color. The color arises when a molecule absorbs certain wavelengths of visible light and transmits or reflects others. Charge transfer complex is the mixture composing of electron donor and acceptor, such that a fraction of electronic charge can be transferred between the molecular entities. The resulting electrostatic attraction provides a stabilizing force for the formation of complexes. By using charge transfer mechanism, the optical properties of chromophores might be finely tuned through the association with polymeric materials for practical application due to the advantage of polymer properties. In contrast to homopolymers, the association of chromophore with BCPs gives the feasibility of forming nanostructured characters for applications. Charge transfer complex between fullerenes and PS-P4VP has been demonstrated so as to give self-assembled nanostructures.[45] Unexpected phase transformation from cylinder to sphere morphology can be found, suggesting that the fullerenes slowly penetrate into the P4VP micellar cores due to charge transfer complexation. Also, the characteristic color change to brown between fullerenes and PS-P4VP has been reported, indicating the optical property variation due to the formation of charge transfer complex.[46]

In this study, we aim to fabricate nanostructured materials with color tuning character by using P4VP-PCL complexed with chromophores possessing the 2-methylidenepropanedinitrile functional group. To achieve the formation of well-defined nanostructured mixtures, a systematic study with respect to the phase behavior of chromophores/P4VP-PCL mixtures is conducted. Owing to the excellent affinity between the chromophore and P4VP block resulting in significant increase on the effective volume fraction of P4VP, phase transformation would be induced by introducing chromophores into the P4VP microdomains so as to result in forming various nanostructures. By taking advantage of the self-assembly of BCPs, the length scale of self-assembled nanostructure is much smaller than the wavelength of visible light so as to give less scattering loss in the visible region. Moreover, homogeneously distributed and higher loading chromophores in polymers can be achieved by mixing chromophores with P4VP-PCL due to the effect of microphase separation whereas the mixing of chromophores with P4VP may encounter segregation problem so as to lower the loading level of chromophores. As a result, for optical application (e.g., color tuning), higher transmittance and color tone can be successfully achieved by mixing chromophores with P4VP-PCL. Also, it is much easier to form uniform thin-film samples for the chromophore/P4VP-PCL mixtures than the chromophore/P4VP mixtures. Accordingly, unlike chromophore/P4VP mixture, transparent thin films of chromophore/P4VP-PCL mixtures can be created, and the appearance of color in the visible region for the mixtures can be fine-tuned by exploiting the bathochromical shifting of charge transfer absorption peaks. Consequently, by taking advantage of transformed morphologies with continuous texture, the association of the chromophores with the P4VP can be varied by tuning pH value so as to give stimuli-responsive, transparent thin films with tunable color.

EXPERIMENTAL SECTION

Materials. Poly(4-vinylpyridine) homopolymer ($M_w \sim 60\,000$) was purchased from Aldrich (St. Louis, MO). A series of P4VP-PCL were synthesized via living ring-opening and atom transfer radical polymerizations in sequence. The molecular characteristics and the sample codes of the P4VP-PCL abbreviated as V*m*C*n* in which *m* and *n* represent the degree of polymerization of each constituted block, respectively, are described in Table 1. The number-average molecular weight (M_n) of V2C7, V4C7, and V5C10 is 9000, 11 000, and 16 540, respectively. The polydispersity index (PDI) determined by gel-permeation chromatography (GPC) with heating DMF column ranges from 1.24 to 1.29. The volume fraction of P4VP ($f_{P4VP}{}^{v}$) was determined by M_ns and densities of P4VP and PCL (0.988 and 1.08 g/cm^3) at which the M_ns of P4VP and PCL were determined by ^{1}H NMR.[17,49]

Nanostructures of P4VP-PCL BCPs. Bulk samples of P4VP-PCL were prepared by solution-casting method using dichloromethane (CH_2Cl_2) solutions (10 wt % of P4VP-PCL) at room temperature. To eliminate possible effects of PCL crystallization and residual solvent on microphase-separated morphology during solvent evaporation, all bulk samples were annealed at 140 °C for 12 h under nitrogen, which is above the glass transition temperature of P4VP block ($T_{g,P4VP} \sim$ 100 °C) and well above the equilibrium melting point ($T_m^{\circ}{}_{,PCL}$ = 69 °C) of PCL block but below estimated order−disorder transition temperature ($T_{ODT} \sim$ 230 °C). After thermal treatment, the samples were rapidly cooled to room temperature at a rate of 150 °C/min. Subsequently, the samples were examined by using TEM and SAXS.[17]

Prepartion of Chromophores/P4VP-PCL Mixtures. 3-(Dicyanomethylidene)indan-1-one (1CN-IN), 1,3-bis(dicyanomethylidene)indan (2CN-IN), tetracyanoquinodimethane (TCNQ), and tetracyanoethylene (TCNE) were used as chromophores to incorporate with the P4VP-PCL so as to give a series of chromophores/P4VP-PCL mixtures for the formation of charge transfer complexes in solution (see Figure 1). By taking advantage of the association between the lone pair in the nitrogen group of P4VP in P4VP-PCL and chromophores, the mixtures can be simply achieved by using dichloromethane (CH_2Cl_2) as solvent at the concentration of 5 wt %. The amount of chromophores introduced was defined by the stoichiometry of chromophores versus nitrogen on the P4VP (marked as chromophore/N)

so as to justify the degree of association. Bulk samples of chromophore/P4VP-PCL mixtures were prepared by solution casting and then thermally treated following similar sample procedure to neat BCP.

Instrumental Details. Differential scanning calorimetry (DSC) experiments were carried out in a Perkin-Elmer DSC 7 equipped with an intracooler and calibrated with cyclohexane and indium for the measurements of thermal behavior of P4VP-PCL. Bright field transmission electron microscopy (TEM) images were obtained using the mass−thickness contrast with a JEOL TEM-1200x transmission electron microscope (at an accelerating voltage of 200 kV). Ultrathin sectioning (50−60 nm) was performed by ultramicrotomy (LEICA ULTRACUT R) with cooling system (LEICA EMFCS) at −100 °C. Staining was accomplished by exposing the samples to the vapor of a 4% aqueous RuO_4 solution for 30 min.

Small-angle X-ray scattering (SAXS) experiments ($\log(q)$ vs q (= $4\pi \sin(\theta/2)/\lambda$); here, q is the scattering vector and θ is the scattering angle) were conducted at the beamline BL17B3 of the National Synchrotron Radiation Research Center (NSRRC). The incident X-ray beam was focused vertically by a mirror and monochromated to the energy of 10 keV by a germanium (111) double-crystal monochromator. The wavelength of the X-ray beam was 1.24 Å. The beam stop was a round tantalum disk 4 mm in diameter. A MAR CCD X-ray detector (MAR USA) was used to collect the two-dimensionsal (2D) SAXS patterns. The scattering angle of the SAXS pattern was calibrated using silver behenate. To eliminate the disturbance of crystallization, all samples were heated over 70 °C ($T_{m,PCL}$ is about 69 °C). For ultraviolet−visble (UV−vis) absorption measurements in solution state, the BCPs samples were dissolved in the dichloromethane (CH_2Cl_2) at room temperature to form 1.0 wt % of P4VP-PCL and chromophore/P4VP-PCL mixture. The absorption spectra in the region of 200−800 nm were recorded by using a Hitachi U-3300 UV−vis spectrophotometer. Fourier transform infrared spectrometer (FTIR) experiments were collected on a Bomem, DA8.3 spectrometer at a resolution of 1 cm^{-1}. The films for FTIR measurements were prepared by casting solution onto 1 cm × 1 cm silcon wafer (100) and dried to prevent the disturbance of water. The experiments were carried out at room temperature (25 °C). To identify the P4VP-PCL associated with chromophore, three-dimensional (3D) GPC analyses,[50,51] consisting of elution column equipped with refractive-index detector and UV/vis spectra in series, were conducted. The 3D GPC measurements consisting of elution column equipped with refractive index detector (Waters 2414 RI detector) and UV/vis spectra (Waters 996 photodiode array detector) in series were performed on Waters 1515 isocratic HPLC pump using THF (HPLC grade) as an eluent. To examine the association strengths of these chromophores with P4VP-PCL, the cyclic voltammetry (CV) was acquired on an electrochemical workstation interfaced and monitored with a PC computer.[52] A three-electrode system consisting of P4VP-PCL associated chromophores spin-coated on FTO-coated (fluorine-doped tin oxide) glass as working electrode, a platinum wire as auxiliary electrode, and an Ag/AgCl as reference electrode was employed. In this study, cyclic voltammogram was carried on CHI627C electrochemical workstation system. Cyclic voltammogram was examined in the voltage windows ranging from −1.5 to 1.5 V (vs Ag/AgCl) at a scan rate of 100 mV s^{-1}, and 3 M KCl acted as an electrolyte.

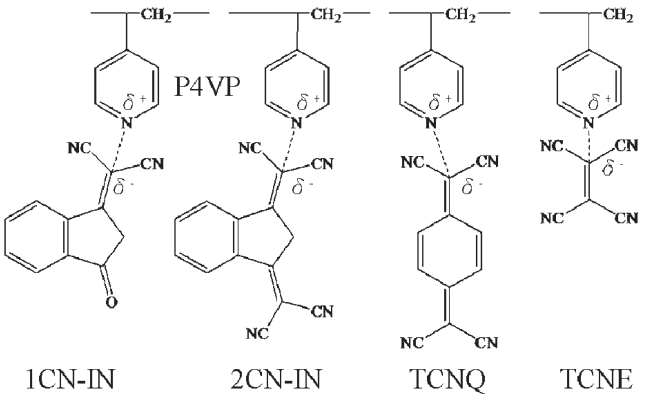

Figure 1. Various chromophores (1CN-IN, 2CN-IN, TCNQ, and TCNE) used for the formation of charge transfer complexes with P4VP.

RESULTS AND DISCUSSION

Association of Chromophores with P4VP. A P4VP homopolymer was used as a model system for the studies of the association of chromophore with BCPs. As shown in Figure 2a, the colors of 1CN-IN and TCNE in CH_2Cl_2 are transparent but purple for 2CN-IN and yellow for TCNQ. While the P4VP homopolymer is introduced into the solutions, the colors of the solutions containing different chromophores turn red for 1CN-IN, indigo for 2CN-IN, yellow for TCNE, and green for TCNQ (Figure 2b); the changes of color suggest the formation of charge transfer complex. To further examine the corresponding changes in color, UV−vis spectra of prepared solutions were acquired. In contrast to the characteristic absorption peaks at 300 nm for 1CN-IN, 350 nm for 2CN-IN, 400 nm for TCNQ, 270 nm for TCNE, and 254 nm for P4VP in CH_2Cl_2, new absorption peaks appears at 480 nm in 1CN-IN/P4VP solution; 530, 580, and 620 nm in 2CN-IN/P4VP solution; 500 and 650 nm in TCNQ/P4VP; 390, 410, and 550 nm in TCNE/P4VP solution can be found (Figure 3). Owing to the formation of charge transfer complex, the charge transfer absorption peaks bathochromically shift due to delocalizing electrons resulting from the increasing number of $\pi-\pi^*$ conjugated electrons of chromophores at which the electron is transferred from pyridine so as to cause

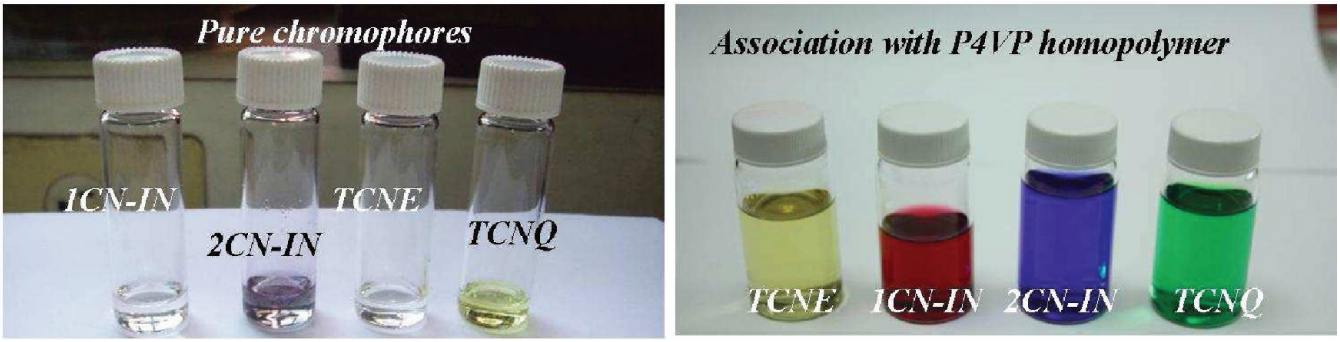

Figure 2. (a) Colors of chromophores dissolved in CH_2Cl_2. (b) Colors of chromophores associated with P4VP homopolymer dissolved in CH_2Cl_2.

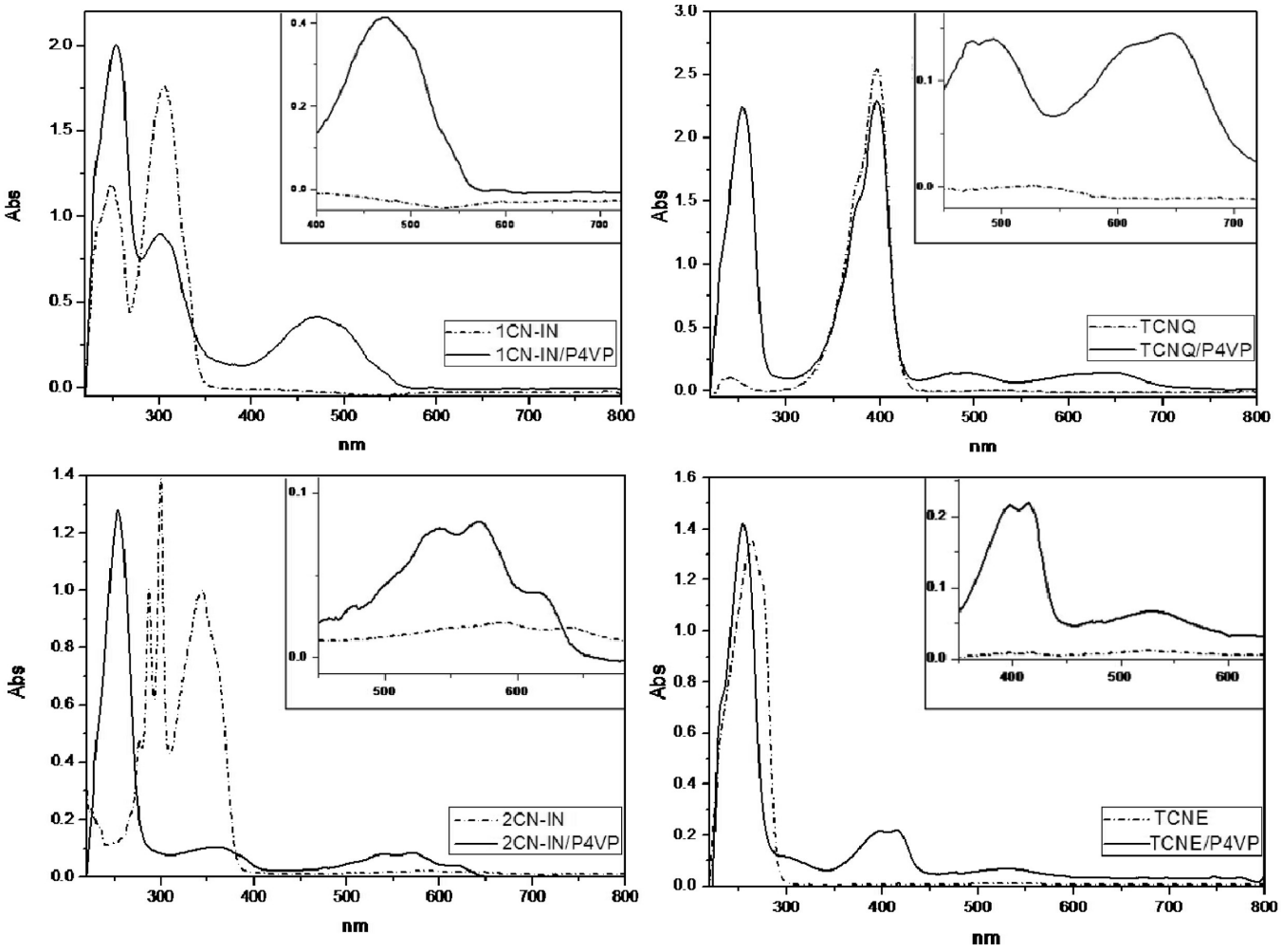

Figure 3. UV−vis spectrum of 1 wt % chromophores/P4VP dissolved in CH_2Cl_2 (straight line) and 1 wt % chromophores dissolved in CH_2Cl_2 (dash-dotted line). Insets show the corresponding enlarged UV−vis spectrum.

the variation in energy gap. As a result, the appearance of the new absorption peaks suggests the occurrence of the charge transfer complex of chromophore and P4VP so that the compensation color of the complexed solution can be visualized.

To further examine the association behavior, FTIR spectra were also acquired. As shown in Figure 4, significant blue shift for the absorption bands at around 1200 (−C═C−) and 1600 cm^{-1} (═N−, pyridine) in the FTIR spectrum can be clearly recognized after the association of chromophore with P4VP. Accordingly, the appearance of extra bands, such as 1260 and 1637 cm^{-1}, in the mixtures of 1CN-IN/P4VP is referred to the association of 2-methylidenepropanedinitrile with pyridine units. Furthermore, the band at 1637 cm^{-1} becomes sharper as compared to 1600 cm^{-1} at higher ratio of 1CN-IN/N, further demonstrating the formation of charge transfer complex (Figure 4a). Similar blue shift results for all of the mixtures examined in this study can be found, reflecting that the color changes are indeed attributed to the association of 2-methylidenepropanedinitrile with the lone-pair electron of nitrogen in P4VP block. In contrast to the chromophores/homopolmer complex system, P4VP-PCL (V5C10) was used for the examination of its association with 1CN-IN. As shown in Figure 4b, similar results with the blue shift of 1600 cm^{-1} can also be observed in the mixtures of 1CN-IN/V5C10, and also the band at 1637 cm^{-1} becomes sharper as compared to 1600 cm^{-1} for the mixtures with higher ratio of 1CN-IN/N. As a result, we suggest that the association of the chromophores with the P4VP block in P4VP-PCL can also be achieved.

Phase Behavior of 1CN-IN/P4VP-PCL Mixtures. To achieve the formation of well-defined nanostructured mixtures, systematic study with respect to the phase behavior of chromophores/P4VP-PCL mixtures was conducted. P4VP-PCL with higher asymmetric constituent composition (that is, V2C7 (f_{P4VP}^{ν} = 0.24)) was used. Different amounts of 1CN-IN chromophores were introduced into P4VP-PCL. Interesting morphological evolution can be observed in the 1CN-IN/V2C7 mixtures (Figure 5). The original cylinder morphology (Figure 5a) can be transformed to lamellar phase while the 1CN-IN/N ratio reaches 1/7, as shown in Figure 5b. With increasing the concentration of 1CN-IN chromophores (ratio of 1CN-IN/N = 1/3), intrinsic microphase-separated lamellar phase gradually transfers to disordered-like phase (Figure 5c), reflecting the occurrence of significant domain swelling after association. Moreover, the evolution of the phase transformation for the 1CN-IN/V2C7 was examined by SAXS experiments (Figure 6). Consistent with the TEM results, the scattering peaks of V2C7 occur at the q^* ratios of $1:2:\sqrt{7}$, suggesting a cylinder phase.

With the introduction of 1CN-IN, the cylindrical characteristic q^* ratios would transfer to lamellar characteristic q^* ratios of 1:2:3

dx.doi.org/10.1021/ma201739b |*Macromolecules* 2011, 44, 8898–8907

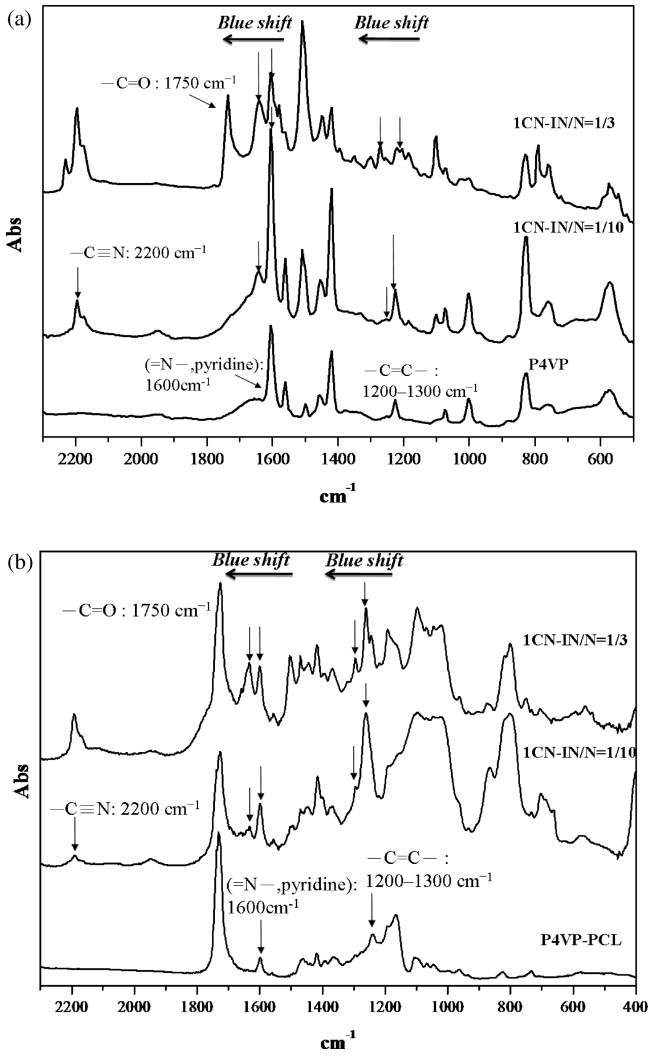

Figure 4. (a) FTIR spectra of P4VP thin-film samples associated with and without 1CN-IN at ratio of 1CN-IN/N = 1/10 and 1/3, respectively. (b) FTIR spectra of V5C10 thin-film samples associated with and without 1CN-IN at ratio of 1CN-IN/N = 1/10 and 1/3, respectively.

at the concentration of the 1CN-IN with 1CN-IN/N = 1/7. Consequently, on the basis of the TEM and SAXS results, the phase transformation from cylinder phase to lamellar phase is a characteristic behavior for the 1CN-IN/P4VP-PCL mixtures. Moreover, for the ratio of 1CN-IN/N = 1/3, the SAXS reflections at the q^* ratio of 1:3 (Figure 6c) can be identified whereas disordered-like lamellae was observed by TEM. Similar to the results of our previous studies in the inorganic/P4VP-PCL hybrids,[17] the lamellar nanostructure can be roughly preserved due to the strong PCL blocking in PCL-rich P4VP-PCL after association with higher ratio of 1CN-IN. Also, consistent to our previous work in inorganic/BCP hybrids,[17] the corresponding changes on morphologies are attributed to the association effect of chromophores with surrounding pyridine chains so as to result in the significant increase of excluded volume. The apparent excluded volume is thus defined as effective excluded volume. Instead of simple swelling by the intrinsic volume of 1CN-IN, the association of the 2-methylidenepropanedinitrile and the lone pair of the nitrogen in the P4VP creates extra volume in the P4VP microdomains so as to lead the phase transformation (see below for reasons).

Effective Excluded Volume. To resolve the effective excluded volume of the 1CN-IN in the mixtures, the volume fraction of complexed P4VP microdomains was calculated by one-dimensional (1D) correlation function from the SAXS results. On the basis of the assumption, the dispersion of the 1CN-IN within the P4VP microdomains is uniformly distributed to form the ideal binary system. By tracing the profile of one-dimensional correlation function, it is convenient to calculate the thicknesses for both complexed P4VP and PCL microdomains. As shown in Figure 7, the plots of the correlation function ($\gamma(z)$) versus real space coordinate (z) data are calculated using one-dimensional correlation function as represented by eq 1:

$$\gamma(z) = \frac{1}{Q}\int_0^\infty q^2 I(q)\cos(qz)\,dq \qquad (1)$$

where $I(q)$ is the one-dimensional intensity; q is the scattering vector.

It is noted that the crystallinity of the PCL may cause the variation of the results of one-dimensional correlation function. To eliminate the disturbance of crystallization, all samples were heated over 70 °C (the melting point of PCL segment is about 69 °C). In the case of the 1CN-IN/V2C7 mixtures (Figure 7), the correlation function reveals that the profile of the hybrids is modified to a symmetric composition. Thus, the thickness of thinner layer and the long period were determined as 8.4 and 18 nm for the mixture with 1CN-IN/N: 1/7 and as 8.7 and 19.4 nm for the mixture with 1CN-IN/N: 1/3. As a result, we suggest that the thinner layer should be referred as the thickness of the PCL microdomain, according to the changes on the long periods for mixtures with 1CN-IN/N: 1/7 and 1CN-IN/N: 1/3 and also the invariant value of ca. 8.4—8.7 nm thickness for the PCL microdomains at different amounts of the 1CN-IN. Obviously, the calculated results represents that the interaction between pyridine and 1CN-IN significantly enhance the excluded volume (see below for details). Interestingly, the swelling of 1CN-IN/V2C7 mixtures reveals different profiles to that of the Au^{3+}/V2C7 hybrids. According to the theoretical prediction on organic molecules/BCP systems, the phase transformation is similar to the results of inorganic/BCP hybrids.[17] Nevertheless, the swelling behavior in Au^{3+}/BCP hybrids is quite different to the chromophore/BCP mixtures at which the phase transformation can be achieved by introducing very small amount of the metal precursors due to the strong association strength of metal ions (Table S2).[17]

Domain Swelling in Various Chromphore/P4VP-PCL Mixtures. To unravel the changes of long periods in V2C7 mixtures with different association strengths of introduced chromophores, the phase transformation and domain swelling induced by charge transfer was examined. For the formation of charge transfer complex, various chromophores including TCNE, 1CN-IN, 2CN-IN, and TCNQ were introduced into the V2C7. In comparison with the TEM images of the V2C7, the 1CN-IN/V2C7, 2CN-IN/V2C7, and TCNQ/V2C7 mixtures all appear as lamellar phase by introducing reasonable amount of chromophores (as illustrated in Figure 8b—d for the ratio of chromophore/N = 1/7). By contrast, for TCNE/V2C7, because of weak association between TCNE and V2C7 (see below for 3D GPC analysis in detail), macrophase separation may occur so that there is no specific morphology forming from the association. The corresponding SAXS results of the mixtures further confirm the identification of lamellar morphologies (Figure 9b—d). Similar

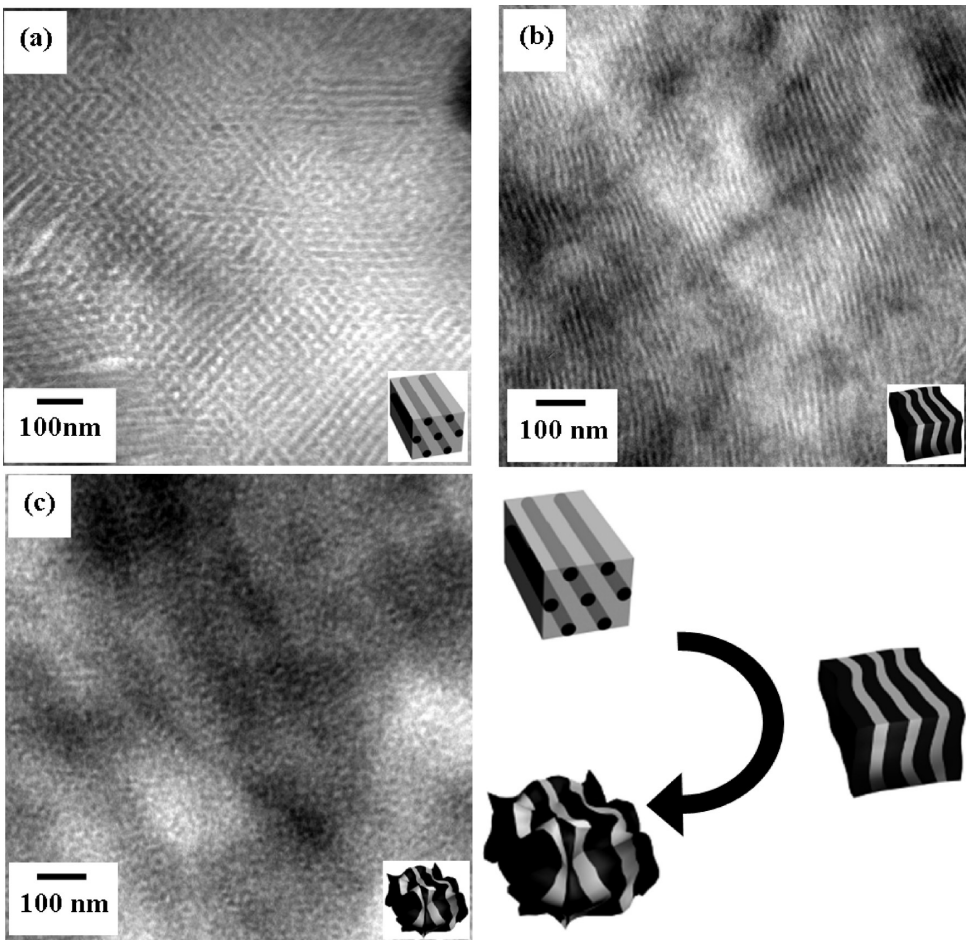

Figure 5. TEM micrographs of (a) V2C7 ($f_{P4VP}{}^{v}$ = 0.24) and its charge transfer complexes at ratio of 1CN-IN/N = (b) 1/7 and (c) 1/3 with RuO_4 staining.

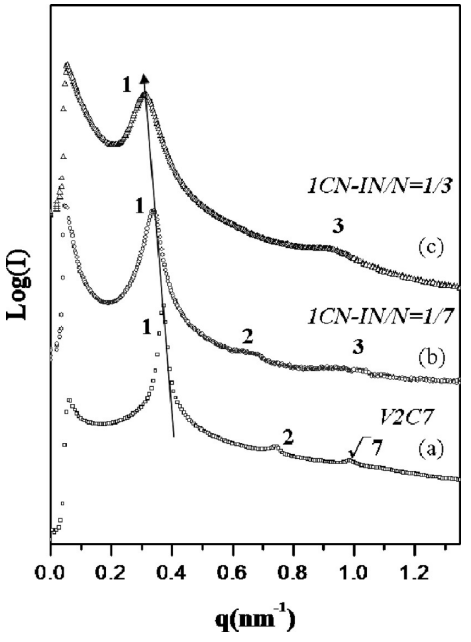

Figure 6. One-dimensional SAXS profiles of (a) V2C7 ($f_{P4VP}{}^{v}$ = 0.24) with different ratios, (b) 1CN-IN/N = 1/7 and (c) 1CN-IN/N = 1/3.

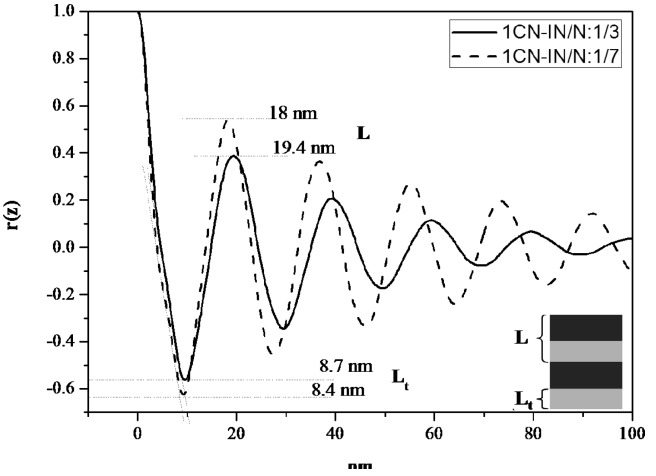

Figure 7. One-dimensional correlation function of 1CN-IN/V2C7 mixtures with different ratios. The thickness of lamellar long period was calculated by the position of first peak, and the average thickness of the thinner layers was determined by the connection between tangent and baseline of the first wave trough.

SAXS results can be found in the association of V4C7 with chromophores (as illustrated in Figure S1 for the ratio of chromophore/N = 1/20). The phase transformation indicates

dx.doi.org/10.1021/ma201739b |*Macromolecules* 2011, 44, 8898–8907

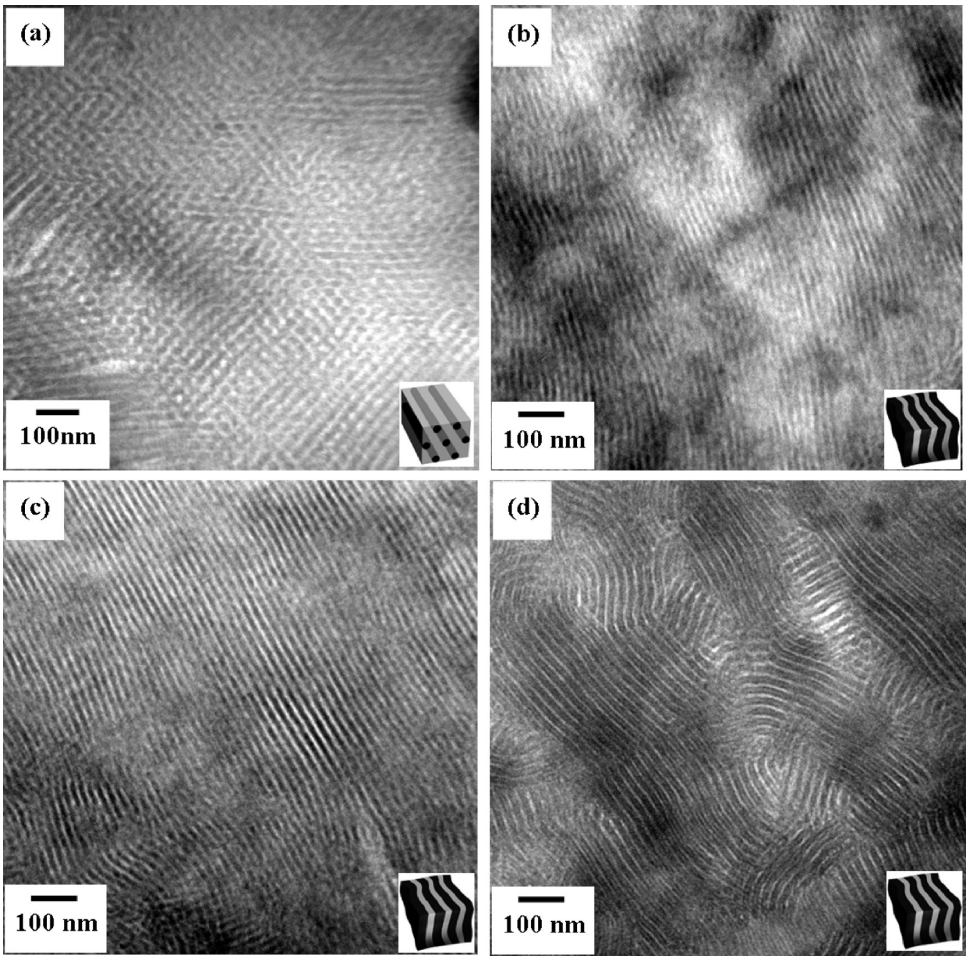

Figure 8. TEM micrographs of (a) V2C7 ($f_{P4VP}^{\nu} = 0.24$) and its charge transfer complexes with (b) 1CN-IN, (c) 2CN-IN, and (d) TCNQ at the ratio of 1/7 with RuO_4 staining.

that the results are in line with the behavior of effective excluded volume as observed previously, reflecting that the introduced chromophores affect the surrounding P4VP chains to lead the increase on excluded volume. In contrast to V2C7 and V4C7 results, the SAXS results of V5C10 association with chromophores show no apparent phase transformation (as illustrated in Figure S2 for the ratio of chromophore/N = 1/10 and 1/3). Furthermore, at higher loading ratio, for V2C7 associated with TCNQ at loading ratio (1/3), the lamellar structure evolves into a cylindrical structure again whereas distorted lamellar morphologies were observed for V2C7 associated 2CN-IN at loading ratio (1/3) (as illustrated in Figure S3). Also, the corresponding TEM results show the cylindrical structure with the PCL block forming the minor phase for V2C7 associated with TCNQ (as illustrated in Figure S4).

We conjecture that the degree of swelling (namely, the contribution of effective excluded volume) would be dependent upon the association strength of the chromophores with the P4VP block. The larger the association strength is, the higher the increase in the swelling degree will be. Namely, the significant swelling is attributed to the enhancement in incompatibility (namely, the interaction parameter). Consequently, significant increase in the effective exclusive volume should be found in the strong association strength so as to lead the phase transformation. Similar behavior with respect to the enhanced interaction

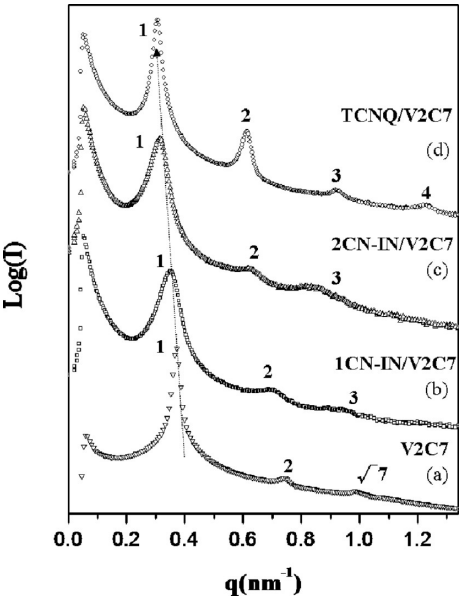

Figure 9. One-dimensional SAXS profiles of (a) V2C7 ($f_{P4VP}^{\nu} = 0.24$) and its mixtures with 1CN-IN, 2CN-IN, and TCNQ at the ratio of 1/7 in (b)−(d), respectively.

dx.doi.org/10.1021/ma201739b |*Macromolecules* 2011, 44, 8898–8907

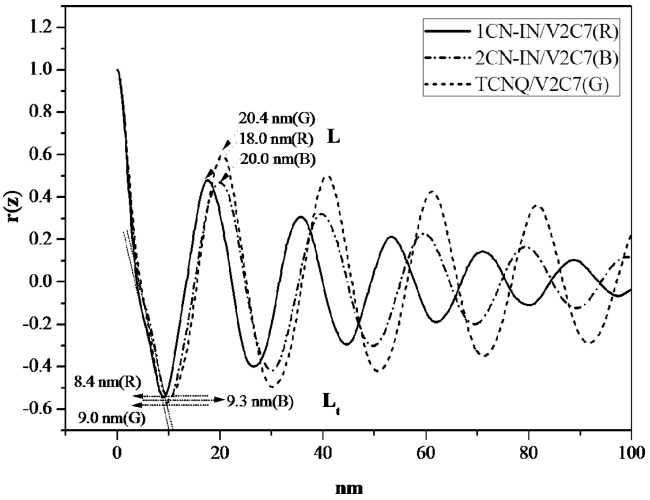

Figure 10. One-dimensional correlation function of chromophores/V2C7 mixtures with 1CN-IN, 2CN-IN, and TCNQ at the ratio of 1/7.

parameter has also been observed in the phase behavior of polystyrene-*b*-poly(methyl methacrylate) (PS−PMMA) complexed with lithium ions at which the occurrence of phase transformation from sphere to cylinders can be found and an increase in spacing of BCP microdomains was identified.[14,15] As mentioned, for the phase transformation of BCP mixtures with strong association, complexed domain chains tend to gain more contact area with associated species and stretching more than the other block at which the enthalpic benefit from strong association is significant enough to compensate the entropic penalty from the complexed domain stretching so as to reduce the total Gibbs free energy of the mixtures. The competition between entropic (chain stretching) and enthalpic energy (association process) thus results in the increase of interaction parameter and effective excluded volume in the BCP mixtures due to the strong association of mixing species with associated block and the stretching of the block chain. Note that it is also possible to cause the stretching of nonassociated block chain due to the stronger repulsion from the complexed block, but the change in dimension should be insignificant. The 1D correlation function results from the SAXS profiles in Figure 10 are summarized in Table 2. The domain spacing (it is marked as d in Table 2) is 16.9 nm for the intrinsic V2C7 but increases to 18, 20, and 20.4 nm after association with the 1CN-IN, 2CN-IN, and TCNQ, respectively. By calculating from 1D correlation function the domain spacing, swelling in PCL is invariant (changing within 1 nm) as expected but the change in P4VP is indeed significant, with the increase from 5 to 7 nm corresponding to different chromophores as listed in Table 2. Also, similar to our previous work,[17,49] the tendency for phase transformation suggesting that effective excluded volume of complexed microdomains (i.e., chromophores/P4VP) can be enhanced by the association between chromophores and the P4VP block as evidenced by 1D SAXS correlation function (it is marked as $f_{excluded}{}^{\nu}$ in Table 2).

In the mixtures with weak association (e.g., the 1CN-IN/P4VP-PCL), the enthalpic benefit from the association is inadequate to overcome the entropic penalty of P4VP chain stretching. As a result, domain swelling in the 1CN-IN/P4VP-PCL mixtures is much smaller than the others. By contrast, for the mixtures with strong association (e.g., the 2CN-IN/P4VP-PCL and TCNQ/P4VP-PCL mixtures), the entropic penalty resulting from P4VP chain stretching can be balanced by the enthalpic benefit due to the association. Accordingly, as compared to the 1CN-IN/P4VP-PCL mixtures, higher domain swelling in the 2CN-IN/P4VP-PCL mixtures is expected. Consequently, we suggest that the origin for distinct domain swelling in various mixtures may result from the balance of enthalpic association and entropic chain stretching. To further examine the association strengths of these chromophores with P4VP-PCL, the cyclic voltammetry (CV) and three-dimensional GPC (3D GPC) were conducted.

Table 2. Characterization of Various Mixtures

sample	ratio	morphology	$f_{P4VP}{}^{\nu}$	$f_{excluded}{}^{\nu}$	interdomain spacing (nm)
V2C7	0	cylinder	0.24	0	16.9
1CN-IN/V2C7(R)	1/7	lamella	0.53	0.27	18
2CN-IN/V2C7(B)	1/7	lamella	0.54	0.30	20
TCNQ/V2C7(G)	1/7	lamella	0.56	0.32	20.4

Figure S5 shows the CV diagram of the P4VP-PCL associated with chromophores. As shown in Figure S5, the reduction potentials of P4VP-PCL associated with 1CN-IN, 2CN-IN, and TCNQ are −0.9, −0.6, and −0.75 V, respectively. As a charge transfer process is one kind of redox reactions, the reduction/oxidation potential is proportional to the change in free energy of the redox reaction (i.e., $\Delta G = -nFE$, where n is number of moles of electrons per mole of product and F is the Faraday constant). Herein, the higher reduction/oxidation potential indicates larger ΔG, resulting in higher energy gap of the redox reaction, so as to further inhibit the charge transfer process. As a result, these results suggest that the association strength follows the order of 2CN-IN > TCNQ > 1CN-IN. Furthermore, by taking advantage of size-extraction effect, the association strength of the charge transfer complex can also be evidenced by 3D GPC. Figures S6−S10 show the 3D GPC analysis of neat P4VP-PCL and P4VP-PCL blended with different chromophores: 1CN-IN, 2CN-IN, TCNQ, and TCNE molecules at the ratio of chromophores/N = 1/3, respectively. The 3D GPC analysis of P4VP-PCL associated with 2CN-IN shows the absorption bands of P4VP-PCL around 220−300 nm, the absorption bands of 2CN-IN molecules around 250−400 nm, and the absorption bands of charge transfer complex of P4VP-PCL with 2CN-IN around 450−650 nm which approximately appear at the same elution time (as illustrated in Figure S8). These results suggest that all of introduced 2CN-IN molecules can be associated with P4VP-PCL so as to form the charge transfer complex. Moreover, the 3D GPC analysis of P4VP-PCL associated with TCNQ or 1CN-IN shows the nonstationary waveform during the elution time which suggests the reversibility and weaker electronic reception of 1CN-IN and TCNQ in comparison with 2CN-IN after association, similar to the CV results. By contrast, Figure S10 shows the 3D GPC analysis of P4VP-PCL associated with TCNE molecules. As found, the absorption bands of P4VP are around 220−300 nm and the ones for TCNE molecules are around 250−400 nm, but they appear at different elution time. These results indicate that weak association between TCNE and V2C7 in comparison with other chromophores. According to the 3D GPC analysis, the association strength follows the order of 2CN-IN > TCNQ and 1CN-IN > TCNE. However, the SAXS analysis indicates that the increase on the degree of domain swelling in various mixtures follows the order of TCNQ ≥ 2CN-IN > 1CN-IN. We speculate that the larger domain swelling in the TCNQ/P4VP-PCL

mixture is attributed to the unique character of TCNQ with high electron affinity of the polyene system conferred by the four cyano groups and the planarity and symmetry of the structure which could form special charge transfer complex between P4VP and TCNQ.[54] In general, TCNQ forms two types of stable, salt-like derivatives in charge transfer complex, each involving complete transfer of an electron to TCNQ with the formation of the anion radical $TCNQ^{\delta-}$. The first type is represented by the simple complex formula $(P4VP^{\delta+})(TCNQ^{\delta-})$. This complex is characterized by intermediate to high resistivity[54] and weak electron paramagnetic resonance absorption.[55] For the second type, the complex can be represented by the formula $(P4VP^{\delta+})[(TCNQ^{\delta-})(TCNQ^{0})]$, containing the neutral TCNQ ($TCNQ^{0}$) in addition to $TCNQ^{\delta-}$ from the other side of 2-methylidenepropanedinitrile, as characterized by exceptionally low electrical resistivity[54] and variable electron paramagnetic resonance.[55] As evidenced by 3D GPC (Figure S9), two kinds of complex in TCNQ/P4VP-PCL solution give rise to the different absorption peaks at 400 and 500 nm with P4VP characteristic peak, indicating that neutral TCNQ may be associated with the $TCNQ^{\delta-}$. Also, the regression of peak at 500 nm over the elution time suggests the extraction of neutral TCNQ following with $(P4VP^{\delta+})(TCNQ^{\delta-})$. On the basis of the special form of $(P4VP^{\delta+})[(TCNQ^{\delta-})(TCNQ^{0})]$, we speculate that the association between P4VP and TCNQ would be dominated by not only the ability of electronic reception but also the volume of $TCNQ^{\delta-}$ containing with neutral TCNQ acting as an attachment larger than that of 2CN-IN. The increase in volume could be contributed by the formation of $(TCNQ^{\delta-})(TCNQ^{0})$ complex so as to lead the formation of lamellar structure, in particular with higher ordering due to the alleviation of bridging effect. Accordingly, the domain swelling increases with the enhancement of association strength and the excluded volume of $(P4VP^{\delta+})[(TCNQ^{\delta-})(TCNQ^{0})]$ in BCP following the order of TCNQ ≥ 2CN-IN, at which the formation of the $(TCNQ^{\delta-})(TCNQ^{0})$ complex gives a larger effective volume as compared to 2CN-IN.

Color Tuning for Charge Transfer Complex Films. By taking advantage of charge transfer, well-defined nanostructured films resulting from mixing of chromophore and P4VP-PCL offer the possibilities to create stimuli-responsive nanomaterials with tunable color. According to the 3D GPC results (see Supporting Information for details), instability between chromophore and P4VP can be observed in the 1CN-IN/P4VP mixtures; i.e., charge transfer complex can be controlled by external forces. It is intuitive to suggest that controlling the association/dissociation processes can be achieved by applying various external stimuli such as temperature, pH, and electric field. In particular, it is noted that the formation of lamellar nanostructure resulting from the transformation of cylinder nanostructure after the association of chromophore with the BCP gives rise to the great opportunity for the control of association/dissociation processes by changing the pH value due to the continuity of the lamellar texture from disoriented microdomains. Consequently, through the introduction of aqueous acid or base solution into the continuous networks, the color change of chromophore/P4VP-PCL mixtures in response to the pH variation of surrounding solution can be achieved. 1CN-IN/V2C7 thin film (the ratio of 1CN-IN/N = 1/7) was prepared and subsequently titrated by aqueous solutions with regulated pH value. The pH of solution was controlled by adding an acid such as $HCl_{(aq)}$ to decrease the pH value and vice versa for $NaOH_{(aq)}$ to increase pH. Figure 11a shows the color change of 1CN-IN/V2C7 thin film from red to transparent during the dissociation process due to the addition of 10 wt % $HCl_{(aq)}$ solution. The reversibility of the color change from transparent to red can also be achieved by adding 10 wt % $NaOH_{(aq)}$ solution onto the film (Figure 11b). We speculate that the dissociation process is might be attributed to the protonation between pyridine and H^+ after adding $HCl_{(aq)}$ solution so as to replace the charge transfer between 2-methylidenepropanedinitrile in the chromophore and the lone-pair electron of nitrogen in P4VP. Conversely, reassociation between chromophore and P4VP can be executed by deprotonation as the pH value is above the pK_a of pyridine after adding $NaOH_{(aq)}$. Systematic studies with respect to the color tuning by using various stimuli for transparent nanostructured thin-film samples are still in progress.

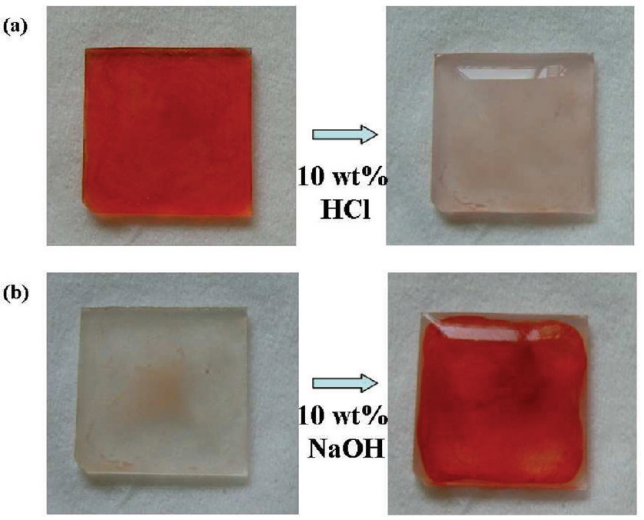

Figure 11. (a) Color change of 1CN-IN/V2C7 thin film at the ratio of 1CN-IN/N = 1/7 from red to transparent after adding 10 wt % $HCl_{(aq)}$ solution. (b) Color change of 1CN-IN/V2C7 thin film from transparent to red after adding 10 wt % $NaOH_{(aq)}$ solution.

CONCLUSIONS

In conclusion, we demonstrated the formation of the mixtures resulting from the association of chromophores with the partial electron transfer from P4VP, as evidenced by FTIR and UV−vis spectroscopic results. Moreover, as observed by TEM, phase transformation can be found by introducing chromophores into P4VP-PCL. The transformation is attributed to the contribution of effective volume fraction due to the association of chromophores with the P4VP block, as evidenced by SAXS. Moreover, the association of the chromophores with the P4VP can be varied by tuning pH value so as to give stimuli-responsive, transparent thin films with tunable color.

ASSOCIATED CONTENT

Supporting Information. Tables S1 and S2 and Figures S1−S10. This material is available free of charge via the Internet at http://pubs.acs.org.

AUTHOR INFORMATION

Corresponding Author

*Tel 886-3-5738349; Fax 886-3-5715408; e-mail rmho@mx.nthu.edu.tw.

REFERENCES

(1) Hamley, I. W. *The Physics of Block Copolymers*; Oxford University Press: New York, 1998.
(2) Bates, F. S.; Fredrickson, G. H. *Phys. Today* **1999**, *52*, 32.
(3) Muthukumar, M.; Ober, C. K.; Thomas, E. L. *Science* **1999**, *277*, 1225.
(4) Fasolka, M. J.; Mayes, A. M. *Annu. Rev. Mater. Res.* **2001**, *31*, 323.
(5) Förster, S.; Plantenberg, T. *Angew. Chem., Int. Ed.* **2002**, *41*, 688.
(6) Hamley, I. W. *Angew. Chem., Int. Ed.* **2003**, *42*, 1692.
(7) Liu, T.; Burger, C.; Chu, B. *Prog. Polym. Sci.* **2003**, *28*, 5.
(8) Park, C.; Yoon, J.; Thomas, E. L. *Polymer* **2003**, *44*, 6725.
(9) Abetz, V.; Simon, P. F. W. *Adv. Polym. Sci.* **2005**, *189*, 125.
(10) Hillmyer, M. A. *Adv. Polym. Sci.* **2005**, *190*, 137.
(11) Tanaka, H.; Hasegawa, H.; Hashimoto, T. *Macromolecules* **1991**, *24*, 240.
(12) Yeh, S. W.; Wei, K. H.; Sun, Y, S.; Jeng, U. S.; Liang, K. S. *Macromolecules* **2005**, *38*, 6559.
(13) Kim, B, J.; Chiu, J. J.; Yi, G. R.; Pine, D. J.; Kramer, E. J. *Adv. Mater.* **2005**, *17*, 2618.
(14) Wang, J. Y.; Chen, W.; Roy, C.; Sievert, J. D.; Russell, T. P. *Macromolecules* **2008**, *41*, 963.
(15) Wang, J. Y.; Chen, W.; Russell, T. P. *Macromolecules* **2008**, *41*, 4904.
(16) Ho, R. M.; Lin, T.; Jhong, M. R.; Chung, T. M.; Ko, B. T.; Chen, Y. C. *Macromolecules* **2005**, *38*, 8607.
(17) Lin, T.; Ho, R. M.; Ho, J. C. *Macromolecules* **2009**, *42*, 742.
(18) Boontongkong, Y.; Cohen, R. E. *Macromolecules* **2002**, *35*, 3647.
(19) Liu, G.; Ding, J.; Hashimoto, T.; Kimishima, K.; Winnik, F. M.; Nigam, S. *Chem. Mater.* **1999**, *11*, 2233.
(20) Boontongkong, Y.; Cohen, R. E.; Rubner, M. F. *Chem. Mater.* **2000**, *12*, 1628.
(21) Moffitt, M.; Vali, H.; Eisenberg, A. *Chem. Mater.* **1998**, *10*, 1021.
(22) Burke, S. E.; Eisenberg, A. *Langmuir* **2001**, *17*, 8341.
(23) Bendejacq, D.; Ponsinet, V.; Joanicot, M.; Loo, Y. -L.; Register, R. A. *Macromolecules* **2002**, *35*, 6645.
(24) Zhang, L.; Eisenberg, A. *Macromolecules* **1996**, *29*, 8805.
(25) Zhang, L.; Shen, H.; Eisenberg, A. *Macromolecules* **1997**, *30*, 1001.
(26) Ma, Y.; Cao, T.; Webber, S. E. *Macromolecules* **1998**, *31*, 1773.
(27) Wang, T. C.; Rubner, M. F.; Cohen, R. E. *Chem. Mater.* **2003**, *15*, 299.
(28) Kuo, S. W.; Wu, C. H.; Chang, F. C. *Macromolecules* **2004**, *37*, 192.
(29) Antoneitti, M.; Wenz, E.; Bronstein, L.; Seregina, M. *Adv. Mater.* **1995**, *7*, 1000.
(30) Seregina, M. V.; Bronstein, L. M.; Platonova, O. A.; Chernyshov, D. M.; Valetsky, P. M. *Chem. Mater.* **1997**, *9*, 923.
(31) Bronstein, L.; Chernyshov, D.; Valetsky, P.; Tkachenko, N.; Lemmetyinen, H.; Hartmann, J.; Forster, S. *Langmuir* **1999**, *15*, 83.
(32) Mossmer, S.; Spatz, J. P.; Moller, M.; Aberle, T.; Schmidt, J.; Burchard, W. *Macromolecules* **2000**, *33*, 4791.
(33) Djalali, R.; Li, S. Y.; Schmidt, M. *Macromolecules* **2002**, *35*, 4282.
(34) Tsutsumi, K.; Funaki, Y.; Hirokawa, Y.; Hashimoto, T. *Langmuir* **1999**, *15*, 5200.
(35) Hashimoto, T.; Harada, M.; Sakamoto, N. *Macromolecules* **1999**, *32*, 6867.
(36) Hashimoto, T.; Okumura, A.; Tanabe, D. *Macromolecules* **2003**, *36*, 7324.
(37) Hashimoto, T.; Tanaka, H.; Hasegawa, H. *Macromolecules* **1990**, *23*, 4378.
(38) Winey, K. I.; Thomas, E. L.; Fetters, L. J. *Macromolecules* **1991**, *24*, 6182.
(39) Shull, K. R.; Mayes, A. M.; Russell, T. P. *Macromolecules* **1993**, *26*, 3929.
(40) He, Y.; Zhu, B.; Inoue, Y. *Prog. Polym. Sci.* **2004**, *29*, 1021.
(41) Sperling, L. H.; Klempner, D.; Utracki, L. A. *Adv. Chem. Ser.* **1994**, *239*, 3.
(42) Jiang, S.; Göpfert, A.; Abetz, V. *Macromolecules* **2003**, *36*, 6171.
(43) Epps, T. H.; Bailey, T. S.; Pham, H. D.; Bates, F. S. *Chem. Mater.* **2002**, *14*, 1706.
(44) Templin, M.; Franck, A.; Chesne, A. D.; Leist, H.; Zhang, Y.; Ulrich, R.; Schadler, V.; Wiesner, U. *Science* **1997**, *278*, 1795.
(45) Ikkala, O.; Osterbacka, R.; Ruokolainen, J. *Macromolecules* **2006**, *39*, 7648.
(46) Fujita, N.; Yamashita, T.; Asai, M.; Shinkai, S. *Angew. Chem., Int. Ed.* **2005**, *44*, 1257.
(47) Moughton, A. O.; O'Reilly, R. K. *J. Am. Chem. Soc.* **2000**, *122*, 474.
(48) Akihiro, O.; Takanori, F.; Katsuhiko, A.; Takuzo, A. *Angew. Chem., Int. Ed.* **2002**, *41*, 3413.
(49) Lin, T.; Li, C. L.; Ho, R. M.; Ho, J. C. *Macromolecules* **2010**, *43*, 3383.
(50) McAlvin, J. E.; Fraser, C. L. *Macromolecules* **1999**, *32*, 6925.
(51) Wu, X.; Fraser, C. L. *Macromolecules* **2000**, *33*, 4053.
(52) Gross-Lannert, R.; Kaim, W.; Olbrich-Deussner, B. *Inorg. Chem.* **1990**, *29*, 5046.
(53) Acker, D. S.; Harder, R. J.; Hertler, W. R.; Mahler, W.; Melby, L. R.; Benson, R. E.; Mochel., W. E. *J. Am. Chem. Soc.* **1960**, *82*, 6408.
(54) Kepler, R. G.; Bierstedt, P. E.; Merrifield, R. E. *Phys. Rev. Lett.* **1960**, *5*, 503.
(55) Chesnut, D. B.; Foster, H.; Phillips, W. D. *J. Chem. Phys.* **1961**, *34*, 684.